



Autism Spectrum Disorder Detection Based on Wavelet Transform of BOLD fMRI Signals Using Pre-trained Convolution Neural Network

Mohammed I. Al-Hiyali¹, Norashikin Yahya^{1*}, Ibrahima Faye¹, Zia Khan¹

¹Centre for Intelligent Signal and Imaging Research (CISIR), Department of Electrical and Electronic Engineering, Universiti Teknologi PETRONAS, Seri Iskandar, Perak, MALAYSIA

*Corresponding Author

DOI: <https://doi.org/10.30880/ijie.2021.13.05.006>

Received 14 April 2021; Accepted 11 May 2021; Available online 31 July 2021

Abstract: Autism spectrum disorder (ASD) is a mental disorder and the main problem in ASD treatment has no definite cure, and one possible option is to control its symptoms. Conventional ASD assessment using questionnaires may not be accurate and required evaluation of trained experts. Several attempts to use resting-state functional magnetic resonance imaging (fMRI) as an assisting tool combined with a classifier have been reported for ASD detection. Still, researchers barely reach an accuracy of 70% for replicated models with independent datasets. Most of the ASD studies have used functional connectivity and structural measurements and ignored the temporal dynamics features of fMRI data analysis. This study aims to present several convolutional neural networks as tools for ASD detection based on temporal dynamic features classification and improve the ASD prediction results. The sample size is 82 subjects (41 ASD and 41 normal cases) collected from three different sites of Autism Brain Imaging Data Exchange (ABIDE). The default mode network (DMN) regions are selected for blood-oxygen-level-dependent (BOLD) signals extraction. The extracted BOLD signals' time-frequency components are converted to scalogram images and used as input for pre-trained convolutional neural networks for feature extraction such as GoogLeNet, DenseNet201, ResNet18, and ResNet101. The extracted features are trained using two classifiers: support vector machine (SVM) and K-nearest neighbours (KNN). The best prediction results are 85.9% accuracy achieved by extracted the features from DenseNet201 network and classified these features by KNN classifier. Comparison with previous studies, has indicated the good potential of the proposed model for diagnosis of ASD cases. From another perspective, the presented method can be applied for analysis of rs-fMRI data on other type of brain disorders.

Keywords: Resting state fMRI, BOLD signal, scalogram, CNN, SVM, KNN, default mode network, ImageNet, transfer learning

1. Introduction

Autism spectrum disorder (ASD) is one of the mental disorders identified by a wide range of symptoms and levels of disability that influences upon person performances and communications with others. The problem in ASD treatment has no definite cure, and one possible option is to control the disorder's progress. In most ASD cases, the diagnosis is only made after the onset of symptoms [1]. ASD symptoms usually appear at around 3-year-old and tend to continue firmly into adolescence and adulthood; therefore, early diagnosis of ASD can play an essential role in addressing above issues and improve the life quality of ASD individuals and their families. A recent study reported in [2] by the United States Centre for Disease Control and Prevention (CDC) showed that 1 in 59 children have ASD in the U.S. The world

*Corresponding author: norashikin_yahya@utp.edu.my

2021 UTHM Publisher. All rights reserved.

penerbit.uthm.edu.my/ojs/index.php/ijie

ASD statistic based on the World Health Organisation (WHO) reports has indicated that 1 in 160 children in the world has ASD [3].

Effective treatments and services can moderate the symptoms and improve the ASD patients' lives, therefore, several studies attempt to use brain imaging modalities for diagnosis and early detection of ASD. The brain imaging modalities such as electroencephalography (EEG), magnetoencephalography (MEG), and functional magnetic resonance imaging (fMRI) are commonly used, especially under resting state term [4]. As a non-invasive tool, fMRI has the best spatial resolution among the methods mentioned above, and it has a sufficient time resolution compared to other methods [5]. The fMRI uses the blood-oxygen-level dependent (BOLD) method to represent the blood flow changes and brain regions' blood oxygenation conditions [6].

In particular, the resting-state fMRI (rs-fMRI) is known to be extensively used to detect functional brain regions. Since the ABIDE dataset availability, many studies have attempted to develop ASD classification models based on rs-fMRI data. For example, Abraham et al. [7] proposed several machine learning frameworks for ASD classification and achieved an accuracy of 66.9%, with a sensitivity rate of 53.2%, and a specificity rate of 78.3% using support vector machine (SVM) classifier. Also, Heinsfeld et al. [8] examined patterns of functional connectivity matrix to optimise the classifier accuracy based on deep learning (DL) networks. The model performance achieved 70% accuracy, 74% sensitivity, and 63% specificity. Recently, Zeinab et al. [9] attempted to improve the automated model performance accuracy for ASD detection by applying a trained functional connectivity matrix with convolution neural network (CNN). Their proposed model achieved 70.22% accuracy, 77% sensitivity, and 61% specificity.

Apart from the above studies, Aghdam et al. [10] proposed an automated model for ASD diagnosis based on structural MRI images using CNN. The best result was accuracy 72%, 71% sensitivity, and 73% specificity. Most of the recent fMRI studies assumed that brain activities are stable during the scanning session and ignored the temporal dynamic features [11]. This supposition may lead to substantial information loss [12, 13]. Although static features reduce the computational complexity by the assumption of activity stability during a time, it might not consider fluctuations in the scan period. Some studies suggested that analysing temporal dynamic features would result in a better distinguishing between normal and abnormal brain activities [14, 15]. The purpose of this study is to present several CNN architectures to diagnose ASD based on temporal dynamic features of BOLD fMRI signals. Moreover, the classification results are improved on a sample of multi-data sources from ABIDE datasets, in which developing the reliability and reproducibility of research outcomes are examined.

2. Material and Method

Several CNN architectures are trained to investigate the autism occurrence in the scalogram images. As shown in the flowchart Fig.1, the BOLD fMRI signals are converted to scalogram images to be the input to four pre-trained CNN architectures to extract the learned features. Furthermore, the extracted features are tested with two classifiers, SVM and KNN for ASD and normal cases classification. Descriptions of the subject method of experiments are explained in the subsequent sections.

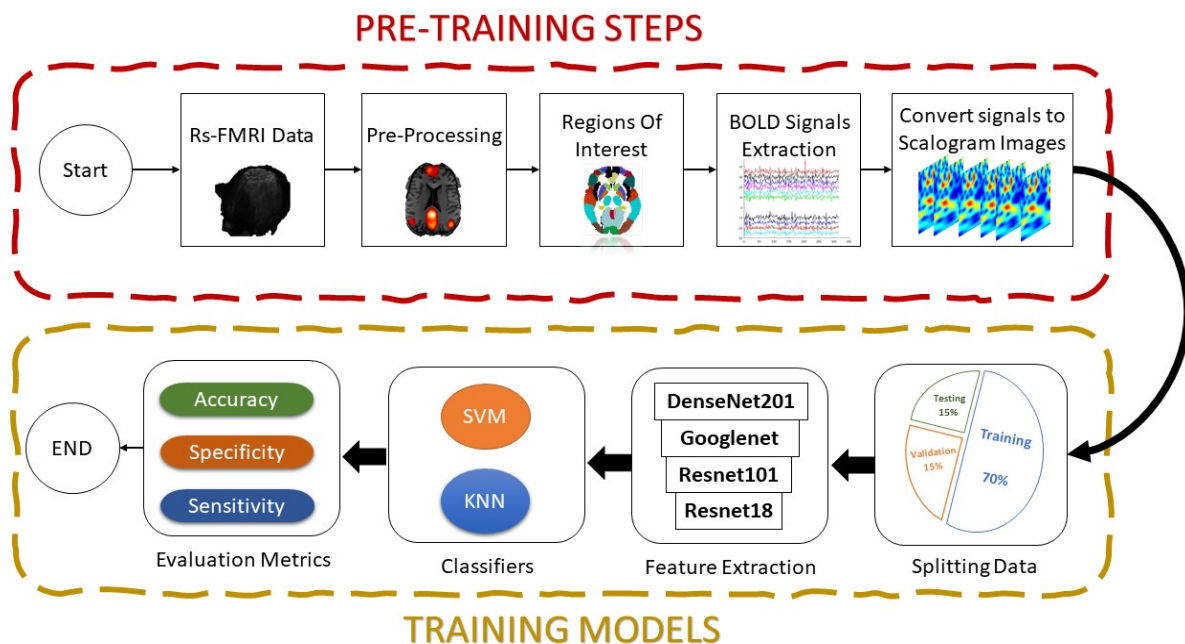


Fig. 1 - General methodology for classification of resting-state BOLD fMRI signals using wavelet transform and pre-trained CNNs

2.1 Subjects

The resting-state fMRI data of 41 ASD and 41 normal control (NC) cases were gathered from the Autism Brain Image Data Exchange (ABIDE) sources [16], taken from multiple independent neuroimaging sites. Detail of the datasets is provided in Table 1.

Table 1 - Sample size and data sources

#	Source	ASD	NC	Sub-Total	Time-point	TR (sec)
1	CALTECH	15	15	30	145	2
2	CMU	14	14	28	315	2
3	KKI	12	12	24	151	2.5
	Total	41	41	82		

Legend: CALTECH: California Institute of Technology, CMU: Carnegie Mellon University, KKI: Kennedy Krieger Institute, TR: Repetition Time

2.2 Data Pre-processing

Like other medical fields data, raw data is typically pre-processed for reduction of noise and artefacts. These steps are crucial before proceeding to the subsequent analyses. The DPARSF is a MATLAB toolbox for fMRI data pre-processing and analysing [17]. In fMRI data, some spikes or ghosting may appear due to electrical instability of an MRI system. Therefore, the first step is performed by discarding the first 5-volume, perceiving only volumes at which the MRI system has reached an equilibrium. The next step is to slice time correction since the differences in the acquisition time of different voxels can be problematic for the analysis of fMRI data. Then, realignment of head motion is performed to remove the mismatch of head location in the time series of images.

Subsequently, spatial normalisation is applied to transform the brain images into a common template space to align the brain size, shape, and orientation across subjects. The functional images are normalised into Montreal neurological institute (MNI) template by using unified segmentation on the T1 images. Then, spatial smoothing is applied with a Gaussian kernel of 8 mm full-width at half-maximum (FWHM) to improve the signal-to-noise ratio (SNR). The automated anatomical labelling (AAL) is selected as the standard brain atlas to divide the brain into 116 regions of interest (ROIs) [18]. The set of ROIs that are worked together in a network varies with cognitive states. The default mode network (DMN) is selected because when a subject is awake and at rest, the DMN is more active than other brain networks [24]. Hence, DMN provides good indication of brain's neuronal activities of ASD subjects, to be extracted in terms of temporal dynamic features. The DMN regions on the right and left hemisphere of human brain are listed in Table 2.

Table 2 - 22 regions of default mode network based on AAL atlas

Label	Anatomical	Label	Anatomical
29	Insula-L	30	Insula-R
31	Cingulum-Ant-L	32	Cingulum-Ant-R
35	Cingulum-Post-L	36	Cingulum-Post-R
37	Hippocampus-L	38	Hippocampus-R
39	ParaHippocampal-L	40	ParaHippocampal-R
55	Fusiform-L	56	Fusiform-R
59	Parietal-Sup-L	60	Parietal-Sup-R
61	Parietal-Inf-L	62	Parietal-Inf-R
65	Angular-L	66	Angular-R
67	Precuneus-L	68	Precuneus-R
85	Temporal-Mid-L	86	Temporal-Mid-R

2.3 Temporal Dynamic Features

First, the time-frequency components are extracted at each signal by using a continuous wavelet transform (CWT). The CWT coefficient is defined as the convolution of the BOLD signal $x(t)$ with the scaled and translated version of the mother wavelet $\varphi_{a,b}(t)$ [20] as shown in equation (1). CWT has become a popular tool in bio-signal analysis [21].

$$CWT(a, b) = \frac{1}{\sqrt{a}} \int_{-\infty}^{\infty} x(t) \cdot \varphi^* \left(\frac{t-b}{a} \right) dt, \quad (1)$$

where variable a denotes wavelet scale, b denotes time shift position and $*$ denotes the complex conjugate [22]. The complex Morlet wavelet is selected as the mother wavelet since Morlet has the best ratio of (1.03) between frequency band and wavelet scale, which helps to interpret results in the frequency domain [20]. By varying the wavelet scale, a and translating along with the localized time index, b one can construct a picture showing both the amplitude of frequency versus the scale. The scalogram image provides the time-frequency components of BOLD signals. Based on the number of DMN regions, the total number of generated scalograms is 22 images/subject giving a total of 1804 images for 82 subjects. The proposed method aims to apply scalogram images as input to pre-trained convolutional neural networks (CNN), which exhibits competitive performance for the ASD detection.

2.4 Feature Extraction using Pre-trained Deep Neural Networks and Classification

Deep learning is at the core of state-of-the-art machine learning models in computer vision applications. Convolutional neural network is one of the essential deep neural building blocks related to the application of local convolution filters for extracting regional information. It is a unique network that has been utilised in medical image analysis that provides excellent support in the improvement of biomedical research [23].

In our study, selected CNN architectures are experimented including ResNet-18 [25], GoogLeNet [21], ResNet-101 [25] and DenseNet-201[26] for features extraction, which was utilised in previous studies with scalogram images [21]. The number of layers of ResNet-18, GoogLeNet, ResNet-101 and DenseNet-201 are respectively 71, 144, 347 and 708-deep. The CNN architectures were pretrained on more than a million images from the ImageNet database [27] for classification into 1000 object categories, such as keyboard, mouse, pencil, and many animals.

The features from the pretrained CNN are obtained from the layer activations of the network. After converting the BOLD signal to scalogram images, the data is split into 70% and 30% for training and testing, respectively. The extracted features from the pre-trained CNN models are obtained. These features are fitted to two classifiers, namely, support vector machine (SVM) and K-nearest neighbours (KNN).

Finally, the performance of each model is evaluated based on evaluation metrics as shown in equations (2-5). Where TP (True Positive) is a definitive score where the model correctly predicts the ASD patients, and TN (True Negative) is a definitive score where the model correctly predicts the normal cases. Conversely, FP (False Positive) is a definitive score where the model incorrectly predicts the ASD patients, and FN (False Negative) is a definitive score where the model incorrectly predicts the normal cases.

$$Accuracy = \frac{TP + TN}{TP + FP + TN + FN} \tag{2}$$

$$Sensitivity = \frac{TP}{TP + FN} \tag{3}$$

$$Precision = \frac{TP}{TP + FP} \tag{4}$$

$$Specificity = \frac{TN}{FP + TN} \tag{5}$$

3. Results and Discussion

In this section, the feature of the scalogram for ASD vs. NC BOLD signals from 22 regions of DMN is first extracted using pretrained CNN architectures and then evaluated using 2 classifiers, SVM and KNN. In the 1st experiment, classification of ASD vs. NC is evaluated using the feature vectors extracted from ResNet-18, GoogLeNet, ResNet-101 and DenseNet-201. The length of feature vectors extracted from each CNN architecture are shown in Table 3. Notably, the length of feature vector depended on the depth of features extraction layer, for instance the feature vector length from 58-layer DenseNet-201 is relatively low compared to another deeper feature extraction layer of ResNet-101, GoogLeNet.

Table 3 - Feature extraction using pre-trained CNN architectures

Pre-trained CNN	Feature extraction layer	Layer number	Total layer	Size of feature vector
ResNet-18	res3b	34	71	$n \times 100352$
GoogLeNet	inception_3a-output	25	144	$n \times 200704$
ResNet-101	res3b	48	347	$n \times 401408$
DenseNet-201	conv3_block1_concat	58	708	$n \times 125440$

n = number of scalograms

The 22 regions of DMN are selected for extraction of the BOLD signals. Figure 2 shows the time series plot of BOLD signal and scalogram images of one DMN region (Insula-L), as an example for an ASD case and NC case. For the classification task, four CNN architectures are trained using the scalogram, and the features from a specific layer as shown in Table 3 are extracted as input to KNN and SVM. The evaluation results based on testing dataset are shown in Table 4. The best performing network for classification of the scalogram images is obtained from DenseNet-201 and input to KNN classifier, with $k=1$. The performance of the model has achieved an accuracy of 86.0%, a sensitivity of 86.0%, and specificity of 86.0%. Hence, the DenseNet201 give the best performance, followed by ResNet-101, GoogLeNet, ResNet-18 because of the feature extraction layer 'conv3_block1_concat' of the DenseNet-201 is located at layer 58 from 708 layers, which is at a deeper layer compared to other CNN architectures. Hence, better feature representation is provided by the DenseNet-201 as evident from the performance results shown in Table 4. The better performance of DenseNet-201 can be attributed to its unique dense block architecture, where each layer receives feature maps from all preceding layers giving features at all complexity levels. Although relatively deep network compared to ResNet, the use of dense block architecture allows the DenseNet-201 to be thinner and compact with a smaller number of parameters than ResNet.

Performance using 3 types of kernel function for SVM and number of neighbourhoods for KNN is tabulated in Table 5 and Table 6, respectively. Based on the performance values evaluated for 3 kernel functions, linear-SVM achieved the best result compared to other kernels. Similar test for KNN is evaluated at 1, 3, and 5-neighbourhood and the results of accuracy, sensitivity and specificity are shown in Table 6 indicates $k=1$ gives the best performance. The subsequent evaluation of the classification model (DenseNet-201+KNN) is based on KNN with a neighbourhood of 1.

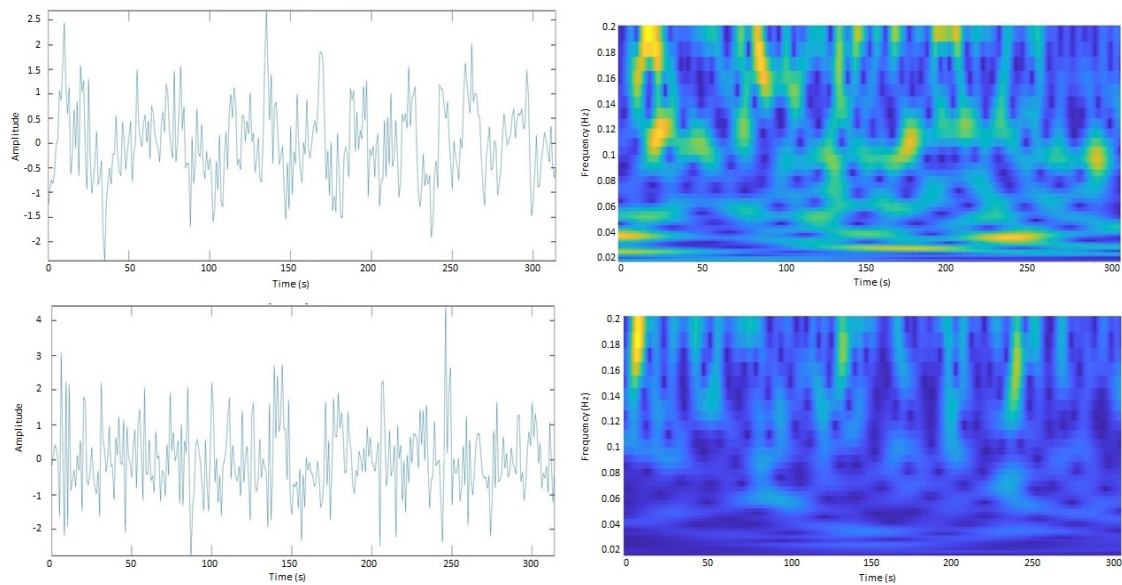


Fig. 2 - Time-series plot of BOLD signals and the corresponding time-frequency scalogram for NC (1st row) and ASD (2nd row)

Table 4 - Percentage of accuracy, sensitivity, specificity for all proposed models based on testing dataset

Pretrained CNN	Classifier	Accuracy	Sensitivity	Specificity
GoogLeNet	KNN	80.0	67.4	97.2
ResNet-18	KNN	77.0	56.4	73.1
ResNet-101	KNN	84.4	73.4	82.4
DenseNet-201	KNN	86.0	86.0	86.0
GoogLeNet	SVM	77.2	65.4	73.2
ResNet-18	SVM	78.0	69.1	80.4
ResNet-101	SVM	77.7	67.1	72.2
DenseNet-201	SVM	75.0	70.6	73.0

The confusion matrix of the best model, DenseNet-201+KNN for classifying scalograms of ASD vs. NC BOLD rs-fMRI signals is depicted in Figure 3 giving 86% testing accuracy. To further test the generalizability of the model to unseen data, the model is evaluated using k -fold cross validation. The performance evaluation of DenseNet-201+KNN for (5, 10, 15, 20)-fold is presented in Table 7. From Table 7, the best accuracy, sensitivity, specificity, and precision is

obtained at 15-fold, at 86.6%, 86.9%, 86.5, and 86.3% respectively. These results provide a good indication of no overfitting and that the model has achieved good generalization to unseen data.

Table 5 - Percentage of accuracy, sensitivity, specificity for DenseNet-201+SVM model with different SVM kernel functions

Kernel	Accuracy	Sensitivity	Specificity
Linear	75.0	70.6	73.0
Polynomial	64.3	29.4	58.4
Gaussian	50.0	0.0	50.0

Table 6 - Percentage of accuracy, sensitivity, specificity for DenseNet-201+KNN model with different nearest neighbour, k value

k-NN	Accuracy	Sensitivity	Specificity
1	86.0	86.0	86.0
3	79.8	81.6	80.9
5	76.8	75.7	76.3

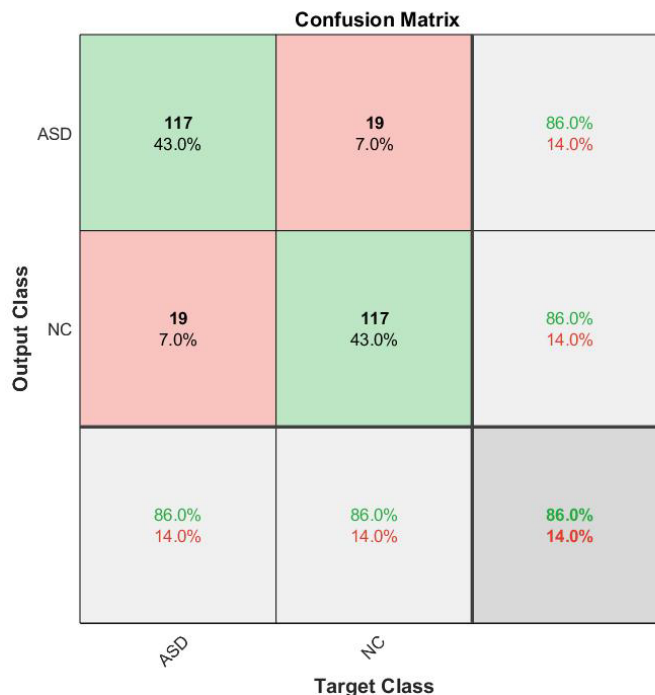


Fig. 3 - Confusion matrix for DenseNet201+KNN model based on testing dataset

The performance comparison of proposed methods with previous studies based on accuracy, sensitivity, and specificity metrics are shown in Table 8. ASD prediction based on Pearson correlation coefficients between BOLD signals [7-9] and of structural MRI images [10] can only yield the highest accuracy of 72.2%, lower to the time-frequency components of BOLD signals. Our proposed method that input CWT of 21 brain regions of DMN to CNN with KNN classifier has shown to result in a good accuracy of 86.6%, that is 13.9% higher than the structural MRI images-based method proposed by Aghdam et al. [10].

Table 7 - Percentage of accuracy, sensitivity, specificity, and precision (± standard deviation) for DenseNet-201+KNN model using k-fold cross-validation

k-fold	Accuracy	Sensitivity	Specificity	precision
5-fold	84.8 ± 1.9	85.0 ± 2.6	84.6 ± 2.1	84.5 ± 2.33
10-fold	86.5 ± 2.4	86.6 ± 3.4	86.6 ± 2.3	86.6 ± 2.5
15-fold	86.6 ± 3.2	86.9 ± 3.5	86.5 ± 4.1	86.3 ± 4.7
20-fold	86.6 ± 3.8	87.1 ± 4.4	86.3 ± 4.5	86.0 ± 5.0

Table 8 - Comparison of the best proposed model with previous studies based on percentage of accuracy, sensitivity and specificity

Method	Subjects #		Accuracy	Sensitivity	Specificity
	ASD	NC			
Abrahman et al. 2017 [7]	871		66.9	53.2	78.3
Heinsfeld et al. 2018 [8]	505	530	70.0	74.0	63.0
Aghdam et al. 2019 [10]	54	62	72.7	71.2	73.4
Sherkatghanad et al. 2020 [9]	871		70.2	77.0	61.0
Our proposed method	41	41	86.6	86.9	86.5

4. Conclusion

In this paper, ASD classification techniques based on temporal dynamic features of BOLD signals from DMN regions and features extracted using pre-trained CNN models are investigated. The temporal dynamic feature of BOLD signal is extracted using wavelet transform, which basically represents the time-frequency component in 2D format, known as scalogram. The scalogram images are fed to selected ImageNet pre-trained CNN models, ResNet-18, GoogLeNet, ResNet-101 and DenseNet-201 for feature extraction. From the feature extraction layer of the CNN models, 1D feature vectors are extracted to be the input of a classifier. Tested on KNN and SVM, the DenseNet-201+KNN yielded the best classification performance and outperformed recently published algorithms. It can be concluded that the DenseNet-201 backend network provides better scalogram features than other networks at the best accuracy of 86.6%. This good performance can be attributed to its densely connected convolutional layer, that provides a deeper network but having thinner and compact architecture with relatively smaller number of trainable parameters. These results have indicated that the proposed methods can be considered as a promising tool for diagnosing ASD and other brain disorders. On a different note, some recommendations for future works are given here; first, the sample size is 82 subjects from three ABIDE data sources might be considered a moderate size. Thus, there is a need to use more subjects to build a more robust model. Secondly, this work only utilized the temporal dynamic features of DMN thus, other brain networks should be considered. Besides, extraction of the dynamic features of BOLD signals such as wavelet coherence transform between brain networks are to be investigated in the future, for better classification of ASD cases.

Acknowledgement

This research is supported by two research grants: (1) the Ministry of Higher Education Malaysia under Higher Institutional Centre of Excellence (HICoE) Scheme awarded to Centre on Intelligent Signal and Imaging Research (CISIR) and (2) the Yayasan Universiti Teknologi Petronas under Grant number YUTP-FRG 015LC0-031.

References

- [1] Grzadzinski, R., Huerta, M., & Lord, C. (2013). (DSM-5) and autism spectrum disorders (ASDs): an opportunity for identifying (ASD) subtypes. *Molecular autism*, 4, 1-6.
- [2] Baio, J., Wiggins, L., Christensen, D. L., Maenner, M. J., Daniels, J., Warren, Z., et al. (2018). Prevalence of autism spectrum disorder among children aged 8 years—autism and developmental disabilities monitoring network, 11 sites, United States, 2014. *MMWR Surveillance Summaries*, 67, 1.
- [3] Elsabbagh, M., Divan, G., Koh, Y.-J., Kim, Y. S., Kauchali, S., Marcín, C., et al. (2012). Global prevalence of autism and other pervasive developmental disorders. *Autism research*, 5, 160-179.
- [4] Hull, J. V., Dokovna, L. B., Jacokes, Z. J., Torgerson, C. M., Irimia, A., & Van Horn, J. D. (2017). Resting-state functional connectivity in autism spectrum disorders: a review. *Frontiers in psychiatry*, 7, 205.
- [5] Crosson, B., Ford, A., McGregor, K. M., Meinzer, M., Cheshkov, S., Li, X., Briggs, R. W. (2010). Functional imaging and related techniques: an introduction for rehabilitation researchers. *Journal of rehabilitation research and development*, 47, vii.
- [6] Fu, Z., Tu, Y., Di, X., Biswal, B. B., Calhoun, V. D., & Zhang, Z. (2017). Associations between functional connectivity dynamics and BOLD dynamics are heterogeneous across brain networks. *Frontiers in human neuroscience*, 11, 593.
- [7] Abraham, A., Milham, M. P., Di Martino, A., Craddock, R. C., Samaras, D., Thirion, B., & Varoquaux, G. (2017). Deriving reproducible biomarkers from multi-site resting-state data: an autism-based example. *NeuroImage*, 147, 736-745.

- [8] Heinsfeld, A. S., Franco, A. R., Craddock, R. C., Buchweitz, A., & Meneguzzi, F. (2018). Identification of autism spectrum disorder using deep learning and the (ABIDE) dataset. *NeuroImage: Clinical*, 17, 16-23.
- [9] Sherkatghanad, Z., Akhondzadeh, M., Salari, S., Zomorodi-Moghadam, M., Abdar, M., Acharya, U. R., et al. (2020). Automated Detection of Autism Spectrum Disorder Using a Convolutional Neural Network. *Frontiers in Neuroscience*, 13, 1325. doi:10.3389/fnins.2019.01325
- [10] Aghdam, M. A., Sharifi, A., & Pedram, M. M. (2019). Diagnosis of Autism Spectrum Disorders in Young Children Based on Resting-State Functional Magnetic Resonance Imaging Data Using Convolutional Neural Networks. *Journal of digital imaging*, 32, 899-918.
- [11] Van Dijk, K. R., Hedden, T., Venkataraman, A., Evans, K. C., Lazar, S. W., & Buckner, R. L. (2010). Intrinsic functional connectivity as a tool for human connectomics: theory, properties, and optimization. *Journal of neurophysiology*, 103, 297-321.
- [12] Hutchison, R. M., Womelsdorf, T., Allen, E. A., Bandettini, P. A., Calhoun, V. D., Corbetta, M., et al. (2013). Dynamic functional connectivity: promise, issues, and interpretations. *Neuroimage*, 80, 360-378.
- [13] Menon, S. S., & Krishnamurthy, K. (2019). A comparison of static and dynamic functional connectivities for identifying subjects and biological sex using intrinsic individual brain connectivity. *Scientific reports*, 9, 1-11.
- [14] Deco, G., Jirsa, V., & Friston, K. J. (2012). The dynamical structural basis of brain activity. *Principles of brain dynamics: Global state interactions*, 1.
- [15] Atasoy, S., Deco, G., Kringelbach, M. L., & Pearson, J. (2018). Harmonic brain modes: a unifying framework for linking space and time in brain dynamics. *The Neuroscientist*, 24, 277-293.
- [16] Craddock, C., Benhajali, Y., Chu, C., Chouinard, F., Evans, A., Jakab, A., et al. (2013). The neuro bureau preprocessing initiative: open sharing of preprocessed neuroimaging data and derivatives. *Frontiers in Neuroinformatics*, 7.
- [17] Yan, C., & Zang, Y. (2010). (DPARF): a MATLAB toolbox for pipeline data analysis of resting-state (fMRI). *Frontiers in systems neuroscience*, 4, 13.
- [18] Tzourio-Mazoyer, N., Landeau, B., Papathanassiou, D., Crivello, F., Etard, O., Delcroix, et al. (2002). Automated anatomical labeling of activations in SPM using a macroscopic anatomical parcellation of the MNI MRI single-subject brain. *Neuroimage*, 15,
- [19] Uddin, L. Q., Supekar, K., Lynch, C. J., Khouzam, A., Phillips, J., Feinstein, C., et al. (2013). Saliency network-based classification and prediction of symptom severity in children with autism. *JAMA psychiatry*, 70, 869-879.
- [20] Torrence, C., & Compo, G. P. (1998). A practical guide to wavelet analysis. *Bulletin of the American Meteorological society*, 79, 61-78.
- [21] Yahya, N., Musa, H., Ong, Z. Y., & Elamvazuthi, I. (2019). Classification of Motor Functions from Electroencephalogram (EEG) Signals Based on an Integrated Method Comprised of Common Spatial Pattern and Wavelet Transform Framework. *Sensors*, 19, 4878.
- [22] Morabito, F. C., Campolo, M., Mammone, N., Versaci, M., Franceschetti, S., Tagliavini, F., et al. (2017). Deep learning representation from electroencephalography of early-stage Creutzfeldt-Jakob disease and features for differentiation from rapidly progressive dementia. *International journal of neural systems*, 27, 1650039.
- [23] Choe, J., Lee, S. M., Do, K.-H., Lee, G., Lee, J.-G., Lee, S. M., & Seo, J. B. (2019). Deep Learning-based Image Conversion of CT Reconstruction Kernels Improves Radiomics Reproducibility for Pulmonary Nodules or Masses. *Radiology*, 292, 365-373.
- [24] Jung, M., Kosaka, H., Saito, D. N., Ishitobi, M., Morita, T., Inohara, K., et al. (2014). Default mode network in young male adults with autism spectrum disorder: relationship with autism spectrum traits. *Molecular autism*, 5(1), 1-11.
- [25] He, K., Zhang, X., Ren, S., & Sun, J. (2016). Deep residual learning for image recognition. In *Proceedings of the IEEE conference on computer vision and pattern recognition* (pp. 770-778).
- [26] Huang, G., Liu, Z., Van Der Maaten, L., & Weinberger, K. Q. (2017). Densely connected convolutional networks. In *Proceedings of the IEEE conference on computer vision and pattern recognition* (pp. 4700-4708).
- [27] Russakovsky, O., Deng, J., Su, H., Krause, J., Satheesh, S., Ma, S., et al. (2015). ImageNet large scale visual recognition challenge. *International journal of computer vision*, 115(3), 211-252.